nature geoscience
SUPPLEMENTARY INFORMATION
DOI: 10.1038/NGEO2075

Appendixes: Hadean age for a post-magma-ocean zircon confirmed by atom-probe tomography

JOHN W. VALLEY, AARON J. CAVOSIE, TAKAYUKI USHIKUBO, DAVID A. REINHARD, DANIEL F. LAWRENCE, DAVID J. LARSON, PETER H. CLIFTON, THOMAS F. KELLY, SIMON A. WILDE, DESMOND E. MOSER, MICHAEL J. SPICUZZA

Appendix 1

Analytical techniques and references for zircon separation, mounting and polishing, imaging, SIMS analysis, and Atom-Probe Tomography.

Appendix 2

Tables of SIMS U-Pb and APT Pb data for zircon 01JH36-69 from the Jack Hills, Western Australia.

Appendix 3

Table of major and trace element compositions measured by APT for inside and outside of clusters from the core of zircon 01JH36-69 from Jack Hills, Western Australia.

Appendix 4

3-D rotating images of Pb (^{207}Pb and ^{206}Pb only) and Y measured by APT in specimen #2 from the core of zircon 01JH36-69 from Jack Hills, Western Australia. Scale in nm with no vertical exaggeration.
App. 4A: atoms of Y including background for the full 1000-nm-long specimen shown in Fig. 3A.
App. 4B: Y & Pb for the enlarged ~100 nm domain shown in Fig. 3B. Only data from within the 3-at.% contour are shown to accentuate clusters.

Appendix 5

Full spectra measured by APT from the core of zircon 01JH36-69 from Jack Hills, Western Australia. Enlarged view of mass 101 to 104.5 showing peaks for $^{206}Pb^{++}$, $^{207}Pb^{++}$, and $^{208}Pb^{++}$ & $^{104}(Si_2O_3)^+$. The peaks for ^{206}Pb and ^{207}Pb are without detectable interferences, whereas Si_2O_3 interference prevents accurate measurements of ^{208}Pb.

Appendix 6

Electron backscatter diffraction (EBSD) measurement of lattice orientation of zircon 01JH36-69 from Jack Hills, Western Australia, with subset of orientation data shown in the area of APT lift outs (specimens) adjacent to a SIMS spot with a date of 4382 Ma. Values of $\delta^{18}O$ correlate to pits shown in Fig. 1C. Green pixels represent high electron diffraction and indexing whereas black pixels could not be indexed as zircon due to topographic effects (fractures, pits, SIMS spots), loss of crystallinity due to radiation damage (correlated to dark disturbed CL zones labelled D in Fig. 1A) and SIMS ablation, or inclusions of phases other than zircon. Note that the a-axis is normal to the section throughout the grain, including the region of interest where crystallographic orientations are uniform (see stereo net plot of poles to {100} from area in Subset 1).

Appendix 7

Oxygen 2-isotope and oxygen 3-isotope data for zircon 01JH36-69 measured at WiscSIMS.

Appendix 1. Analytical technique and references for zircon separation, mounting and polishing, imaging, SIMS analysis, and Atom-Probe Tomography.

Sample 01JH36-69 is a detrital zircon ($ZrSiO_4$) recovered by electric pulse disaggregation of metamorphosed sandstone from the Jack Hills, Western Australia[12,20]. The zircon was cast in epoxy and polished four times revealing surfaces successively deeper into the 230 x 230 x 430 μm prismatic crystal (Fig. 1). Surfaces 1 and 2 were shallow, only revealing the outer portion of the grain. This study reports new data from surfaces 3 and 4, which are closely spaced and exposed the core of the zircon for the first time. These surfaces were imaged by scanning electron microscopy (SEM) and analyzed by secondary ion mass spectrometry (SIMS) in 10 to 20 μm diameter spots, 1 to a few μm deep, to determine the age, stable isotope ratios, and trace element compositions. Surface 4 was analyzed by electron backscatter diffraction (EBSD). Needle-shaped specimens of zircon were prepared using standard site-specific focused ion beam (FIB) methods to dimensions of ca. 100 x 100 x up to 1000 nm for atom probe analysis; up to 4×10^8 ions/ specimen were field evaporated into a time-of-flight mass spectrometer and located at sub-nanometer scale by a position-sensitive detector with an efficiency of ~37%.

Surface 3 of zircon 01JH36-69 was analyzed to determine the U-Pb age using the SHRIMP II ion microprobe at Curtin University with methodology outlined previously[20,28]. Age determinations involved 7 measurement cycles for each mass, and were calibrated using zircon U-Pb standard CZ3 (age = 564 Ma; U = 551ppm)[29]. Grains of CZ3 were located within the same epoxy mount as the sample. Five analyses of CZ3 were made, using a 'bracketing strategy', whereby standard analyses were made before, during (between sample analyses #3 and #4), and after analyses of grain 01JH36-69. Data were reduced using the program Squid[30]; sample analyses were corrected for common Pb using measured ^{204}Pb. The 2σ uncertainty in the mean of the Pb/U ratio for the standard analyses was 0.55%. Graphical representations of the U-Pb data were prepared using the program Isoplot[31].

Surface 4 of zircon 01JH36-69 was analyzed in multiple SIMS sessions to determine the oxygen three-isotope ratios[26,27,32] (IMS-1280, UW-Madison, δ^{18}O, δ^{17}O); and trace element composition[33] (IMS-1280, UW-Madison). The analytical techniques of each analysis are reported in these papers. EBSD mapping was performed after SIMS analysis using a Hitachi SU-6600 and Oxford HKL camera (at the University of Western Ontario ZAPLab) at an accelerating voltage of 20kV and step size of 200 nm. No noise reduction of raw data was performed beyond wildspike correction.

Atom Probe measurements were made using a LEAP 4000X HR® at the CAMECA Atom Probe Technology Center, Madison, Wisconsin. Zircon slices measuring ~3 x 30 μm were removed from the polished face of the crystal and milled to needle-like specimens using a FIB guided by SEM and CL (Fig. 1). Six specimens were obtained from one FIB lift out (Fig. 1A,C). The orientation of each specimen is normal to, and pointing towards, the polished surface in the (100) plane.

The local electrode atom probe (LEAP) is described in detail elsewhere[6,34-36]. Using a LEAP, equipped with laser pulsing capability[37], analysis of bulk insulators has recently become a standard capability[38]. In this instrument, the specimen is a sharp needle cooled to 50K at high vacuum and a high voltage (typically 4-14 kV) is applied. In this study, a 355 nm wavelength laser (pulse energy 400 pJ, pulsed at 200 kHz) was focused on the specimen to promote field evaporation of, on average, approximately 0.008 ions/ pulse. Ions travel through a time-of-flight mass spectrometer and are recorded by a position-sensitive detector. Each laser pulse starts the clock for time-of-flight. For the specimens used in this study (which measure ~100 nm in diameter), the spatial resolution of detected atoms is ±0.3 nm in X-Y-Z coordinates. A total of 6 $x10^8$ ions were detected; 2 $x10^8$ from specimen #1 (R52 126841) and 4 $x10^8$ from specimen #2 (R52 126859) at rates of $\sim 10^7$ ions/hour. In principle, all ions are detected with an equal efficiency of ~37% and a minimum detection limit, determined primarily by the volume of the analysis, of 10 ppma (atomic) for these data. However, spectra must be individually evaluated as some elements ionize poorly or form ionized molecules and isobaric interferences. Mass resolving power is ~1000 (FWHM).

28. Williams, I. S. U–Th–Pb geochronology by ion microprobe. In: McKibben, M.A., Shanks III, W.C., Ridley, W.I. (Eds.), Applications of Microanalytical Techniques to Understanding Mineralizing Processes. *Rev. Econ. Geol*. **7**, 1–35 (1998)
29. Pidgeon, R. T., Furfaro, D., Kennedy, A. K., Nemchin, A. A., Van Bronswjk, W. Calibration of zircon standards for the Curtin SHRIMP II. *United States Geol. Surv. Circ.* **1107**, 251 (abstract) (1994)
30. Ludwig, K. R. User's Manual for Isoplot/Ex rev. 2.49: A Geochronological Toolkit for Microsoft Excel. *Berkeley Geochronological Center Special Publication* No. 1a. (2001a)
31. Ludwig, K. R. SQUID 1.02, A User's Manual. *Berkeley Geochronological Center Special Publication* No. 2. (2001b)
32. Kita N. T., Ushikubo, T., Fu, B. & Valley, J. W. High precision SIMS oxygen isotope analyses and the effect of sample topography. *Chem. Geol.* **264**, 43-57 (2009)
33. Page F. Z., Fu B., Kita N. T., Fournelle J., Spicuzza M. J., Schulze D. J., Viljoen V., Basei M. A. S., Valley J. W. Zircons from kimberlites: New insights from oxygen isotopes, trace elements, and Ti in zircon thermometry. *Geochim. Cosmochim. Acta*, **71**, 3887-3903 (2007)
34. Kelly, T. F. & Larson D. J. Atom Probe Tomography 2012. *Ann. Rev. Materials Res.* **42**, 1-31 (2012)
35. Larson, D.J., Prosa, T.J., Ulfig R.M., Geiser B.P., Kelly, T.F. Local Electrode Atom Probe Tomography: A User's Guide. Springer (2013)
36. Hellman, O.C., Vandenbroucke, J.A., Rusing, J., Isheim, D. & Seidman, D.N. Analysis of Three-dimensional Atom-probe Data by the Proximity Histogram. *Microsc. Microanal*. **6,** 437–444 (2000).
37. Kellogg, G.L. & Tsong, T.T. Pulsed-laser atom-probe field-ion microscopy. *J. Applied Phys.* **51**(2), 1184-1194 (1980)
38. Larson, D.J., Alvis, R.A., Lawrence, D.F., Prosa, T.J., Ulfig, R.M., Reinhard, D.A., Clifton, P.H., Gerstl, S.S.A., Bunton, J.H., Lenz, D.R., Kelly, T.F., Stiller, K. Analysis of Bulk Dielectrics with Atom Probe Tomography. *Microscopy and Microanalysis* **14**(S2), 1254-1255 (2008)

App. 2A. Summary of U-Th-Pb data and age measured by SIMS for surface 3 of zircon 01JH36-69.

Spot	grain area	U (ppm)	Th (ppm)	Th/U	$^{206}Pb^*/^{238}U$ age (Ma)	1s err	$^{207}Pb^*/^{206}Pb$ age (Ma)	1s err	$^{208}Pb^*/^{232}Th$ age (Ma)	1s err	% conc.
1	core	140	92	0.68	4412	25	4382	5	4445	47	101
2	core	138	95	0.71	4349	24	4365	5	4374	52	100
3	core	93	66	0.74	4391	29	4374	6	4384	61	100
4	rim	61	16	0.27	3436	42	3379	13	3050	147	102
5	rim	119	189	1.64	2798	19	3391	12	492	26	83
6	rim	58	43	0.77	3053	32	3430	16	1206	62	89

App. 2B. Full U-Th-Pb data and age measured by SIMS for surface 3 of zircon 01JH36-69.

Pit	grain area	% comm ^{206}Pb	$^{204}Pb/^{206}Pb$	% err	$^{208}Pb^*/^{232}Th$	% err	$^{208}Pb/^{206}Pb$	% err	$^{207}Pb^*/^{206}Pb^*$	% err	$^{207}Pb^*/^{235}U$	% err	$^{206}Pb^*/^{238}U$	% err	err corr
1	core	0.03	0.00002	45.58	0.2460	1.05	0.1702	0.67	0.55039	0.35	74.57	0.86	0.9826	0.78	0.9111
2	core	0.11	0.00007	28.94	0.2416	1.20	0.1813	0.82	0.54389	0.36	72.23	0.85	0.9632	0.77	0.9074
3	core	0.15	0.00010	9.31	0.2422	1.40	0.1857	1.03	0.54745	0.42	73.69	1.02	0.9763	0.92	0.9086
4	rim	0.44	0.00027	25.82	0.1629	4.82	0.0730	1.75	0.28282	0.83	27.46	1.80	0.7041	1.59	0.8859
5	rim	0.97	0.00061	14.59	0.0247	5.28	0.0954	1.42	0.28505	0.78	21.36	1.15	0.5435	0.85	0.7372
6	rim	0.58	0.00036	26.73	0.0615	5.18	0.0910	1.88	0.29235	1.00	24.42	1.66	0.6058	1.33	0.7983

App. 2C. Background-corrected atoms of Pb detected and $^{207}Pb/^{206}Pb$ measured by APT in two specimens (~0.02μm^3) from the 4374 Ma core of zircon 01JH36-69. Pb-rich clusters concentrate Pb, Y and REEs. Cluster interiors are defined by contours of Y >3 at.% and areas outside of clusters by Y <1 at.%.

Region	^{206}Pb	^{207}Pb	$^{207}Pb/^{206}Pb$	2 SD
Full volume	10,255	5,336	0.52	0.040
Cores of clusters (Y >3%)	2,345	2942	1.25	0.049
Outside clusters (Y <1%)	7,439	2,223	0.30	0.048

App. 3. Trace elements detected by APT in the core of zircon 01JH36-69.

Element	Matrix	Clusters
Zr at. %	18.5	14.0
Si at. %	17.3	16.5
O at. %	63.8	62.2
Hf ppma	1000	1000
P ppma	1000	2000
Y ppma	500	44000
Al ppma	10	300
Li ppma	70	30
Ca ppma	20	30
Mn ppma	7	60
Mg ppma	8	50
Pb ppma	20	800
U ppma	30	nd
Lu ppma	nd	1000
Yb ppma	30	9000
Tm ppma	9	1000
Er ppma	nd	7000
Ho ppma	nd	700
Dy ppma	nd	4000
Tb ppma	nd	60
Gd ppma	nd	1000

nd = not detected

ppma = atoms x 10^{-6}

App. 5

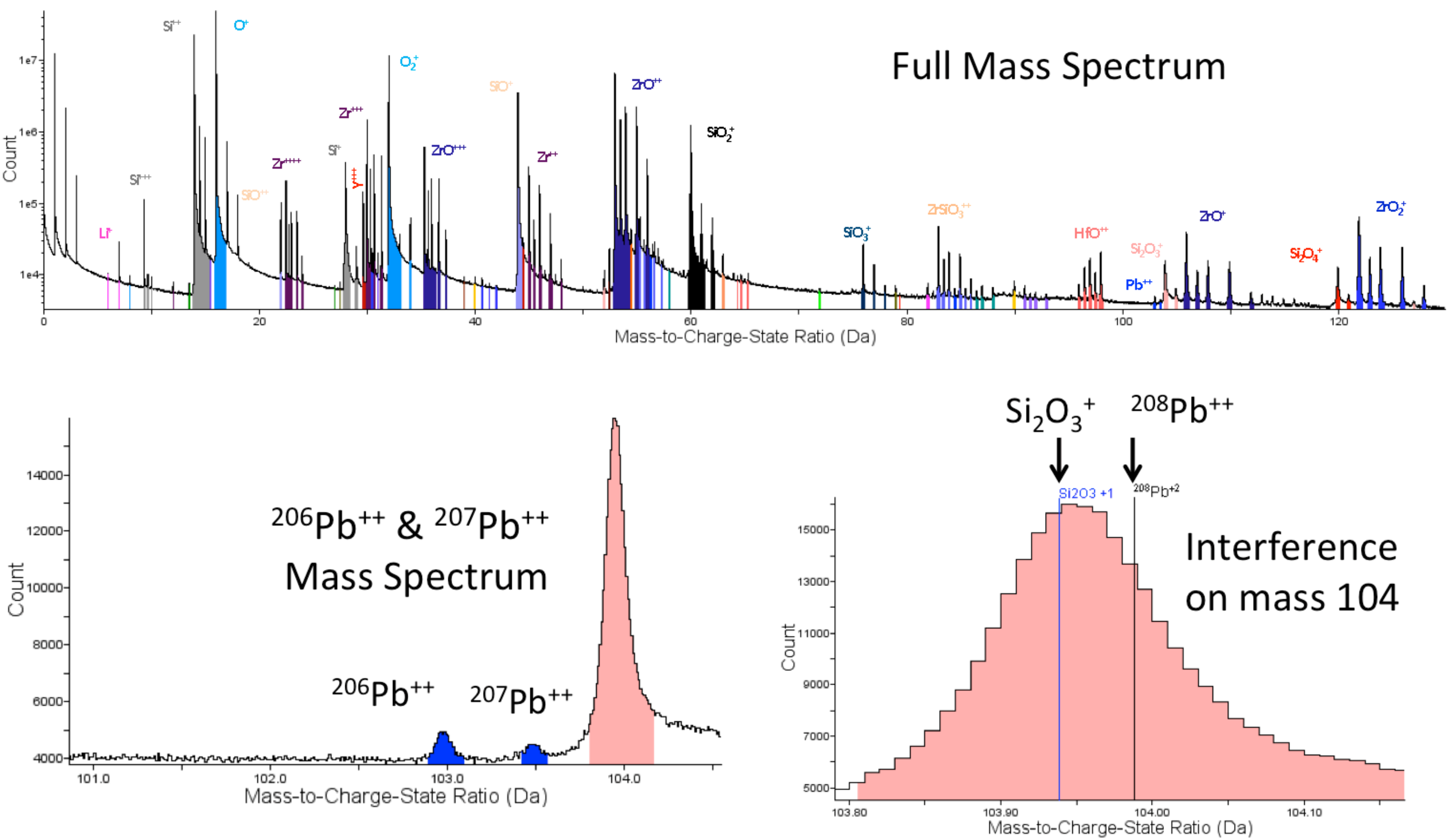
Full Mass Spectrum
Count
Mass-to-Charge-State Ratio (Da)
Li^+
Si^{++}
Si^+
O^+
SiO^{++}
Zr^{++++}
Zr^{+++}
Y^{+++}
O_2^+
ZrO^{+++}
SiO^+
Zr^{++}
ZrO^{++}
SiO_2^+
SiO_3^+
$ZrSiO_3^{++}$
HfO^{++}
$Si_2O_3^+$
Pb^{++}
ZrO^+
$Si_2O_4^+$
ZrO_2^+
$^{206}Pb^{++}$ & $^{207}Pb^{++}$
Mass Spectrum
$^{206}Pb^{++}$
$^{207}Pb^{++}$
$Si_2O_3^+$
$^{208}Pb^{++}$
Si2O3 +1
$^{208}Pb^{+2}$
Interference
on mass 104

App. 6 EBSD measurements of orientation and crystallinity